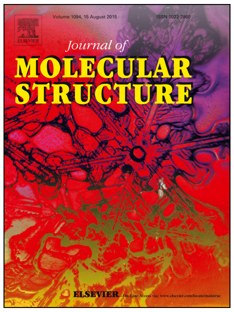

Synthesis, structural, spectral (FT-IR, ^{1}H and ^{13}C-NMR and UV-*Vis*), NBO and first order hyperpolarizability analysis of N-(4-nitrophenyl)-2, 2-dibenzoylacetamide by density functional theory

Şerife Pınar Yalçın, Ümit Ceylan, Ahmet Oral Sarıoğlu, Mehmet Sönmez, Muhittin Aygün

PII: S0022-2860(15)30061-2

DOI: 10.1016/j.molstruc.2015.06.036

Reference: MOLSTR 21588

To appear in: *Journal of Molecular Structure*

Received Date: 13 April 2015

Revised Date: 10 June 2015

Accepted Date: 11 June 2015

Please cite this article as: Ş.P. Yalçın, Ü. Ceylan, A.O. Sarıoğlu, M. Sönmez, M. Aygün, Synthesis, structural, spectral (FT-IR, ^{1}H and ^{13}C-NMR and UV-*Vis*), NBO and first order hyperpolarizability analysis of N-(4-nitrophenyl)-2, 2-dibenzoylacetamide by density functional theory, *Journal of Molecular Structure* (2015), doi: 10.1016/j.molstruc.2015.06.036.

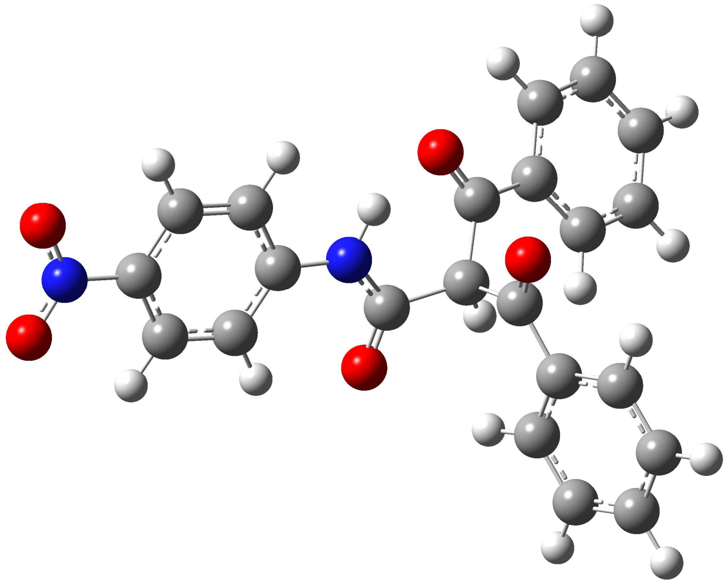

Synthesis, structural, spectral (FT-IR, ^{1}H and ^{13}C-NMR and UV-*Vis*), NBO and first order hyperpolarizability analysis of N-(4-nitrophenyl)-2, 2-dibenzoylacetamide by density functional theory

Şerife Pınar Yalçın[a], Ümit Ceylan[b]✉, Ahmet Oral Sarıoğlu[c],
Mehmet Sönmez[c], MuhittinAygün[d]

[a]*Central Laboratory, Osmanbey Campus, Harran University, 63190 Şanlıurfa, TURKEY*
[b]*Department of Medical Services and Techniques, Vocational High School of Health Services, Giresun University, 28100Giresun, TURKEY*
[c]*Department of Chemistry, Faculty of arts and Sciences, Gaziantep University, 27310, Gaziantep, TURKEY*
[d]*Department of Physics, Faculty of arts and Sciences, DokuzEylül University,Buca,35150, Izmir, TURKEY*

Abstract

The title compound, $C_{22}H_{16}N_2O_5$, was synthesized and characterized by experimental techniques (FT-IR, ^{1}H-NMR, ^{13}C-NMR, UV-Vis and X-Ray single crystal determination) and theoretical calculations. The molecular geometry, vibrational frequencies, molecular electrostatic potential (MEP), thermodynamic properties, the dipole moments, HOMO-LUMO energy has been calculated by using the Density Functional Theory (DFT) method with 6-311G(d,p) and 6-311++G(d,p) basis sets. ^{1}H and ^{13}C-NMR chemical shifts show good agreement with experimental values. According to calculated results, the 6-311G(d,p) and 6-311++G(d,p) basis sets have showed similar results. The optimized geometry can well reproduce the crystal structure parameters.

Keywords: X-ray diffraction; Density functional theory; Quantum chemical calculations; Carboxamide; Characterization.

✉**Corresponding author Tel.:** +90 505 313 51 57

E-mail: umit.ceylan@giresun.edu.tr (Ü. Ceylan); msonmez@gantep.edu.tr, (M. Sönmez)

Introduction

The synthesis, study of structure and properties of amide compounds has been an important research topic during the last several decades [1]. Pyridine carboxamide compounds containing common carboxamide [-C(O)NH-] group in the main structure of proteins are important for construction of metal complexes [2]. These compounds are widely used in the many fields of science such as industrial, pharmacological and biological studies [3-4]. The literature concerning the dibenzoyl acetic acid compounds with nitrophenyl amide is rich and the papers published cover such subjects as synthesize [5], NMR and vibrational characteristics [6,7].

Many important physicochemical properties of biological and chemical systems, investigation of structural properties and theoretical modeling of drug functional material can be predicted by various computational techniques [8,9]. The density functional theory (DFT) and Becke's three-parameter hybrid functional (B3LYP) has been used to determined of molecular structure and vibrational spectra because of its accuracy and consistency with experimental data [10-15].

In this study, the title compound was synthesized as different from the litarature [5], and determined of the molecular geometry, vibrational spectra and assignments, electronic absorption spectra, molecular electrostatic potential, thermodynamic properties. This structure was compared with experimental by ^{1}H-NMR, ^{13}C-NMR, FT-IR and UV-*Vis* spectral methods. In addition, molecular electrostatic potential (MEP), molecular orbital (MO) andnatural bond orbital (NBO) analysis of the title compound were performed by the B3LYP/6-311++G (d,p) level.

Experimental and Computational Methods

Materials and Methods

All the chemicals were obtained from commercial suppliers (Sigma-Aldrich, Merck) and used without any further purification. Elemental analysis (C, H, N, S) was recorded on a Thermo Scientific Flash 2000 elemental analyzer. FT-IR spectra were recorded on a Perkin–Elmer FT-IR type 1650 spectrophotometer. Electronic absorption spectra were recorded in DMF from 1100 to 190 nm range on a PG Instruments T80+UV/Vis spectrometer in ethanol and methanol. ^{1}H-NMR and ^{13}C-NMR spectra were recorded at 25 ^{o}C using an Agilent-

VNMRS-400 spectrometer operating at 400 MHz and 100 MHz respectively. Melting points were measured on a RY-1 micro melting point apparatus.

Synthesis of the N-carboxamide Ligand (H_2L):

A mixture of dibenzoyl acetic acid-*N*-carboxy alkyl amide [8] (339 mg, 1 mmol) and 4-nitroaniline (135 mg, 1 mmol) was stirred at 100 °C for further 3 h in toluene (20 mL). The toluene was removed under vacuum. 50 mL of dry diethyl ether was added to the residue. The solid was filtered, washed with diethyl ether and recrystallized from a mixture of *n*-BuOH/THF. *Anal.Calc*. for $C_{22}H_{16}N_2O_5$: C, 68.04; H, 4.15; N, 7.21. Found: C, 67.81; H, 4.39; N, 7.17. LC-MS/MS (m/z): 389.1 $[M+H]^+$.

Crystal structure determination

The data of the title single crystal was collected via a Agilent Diffraction Xcalibur [16] diffractometer by the ω-scanning technique using graphite-monochromatic MoK_α radiation (λ=0.71073 Å). The intensity symmetries indicate the monoclinic $P12_1/c1$ space group with a = 10.023 (2) Å, b = 21.587 (5) Å, c= 9.401 (2) Å and β = 110.29 (3)°, and Z = 4 in the unit cell. Intensity data were collected in the θ range 5.96-52.72° at 296 K. The structure was solved by direct methods using SHELXS-97 [17] implement in WINGX [18] program suite. The program ORTEP-3 for Windows [19] was used in the preparation of the molecular graphics. The refinement was carried out by full-matrix least-squares method on the positional and anisotropic temperature parameters of the non-hydrogen atoms using SHELXL-97 [20].All H atoms were positioned geometrically and treated using a riding model, fixing the bond lengths at 0.86 and 0.93 Å for NH and CH atoms, respectively. The crystal structure was refined to R=0.097 by the condition of the $I>2\sigma(I)$ threshold. The crystal data, some details data collection conditions and parameters of the refinement process are listed in Table 1, whereas selected bond lengths, bond angles, and torsion angles are shown in Table 2. Full crystallographic data are available as supplementary material.

(Table 1)

Computational details

All theoretical calculations were conducted using Density Functional Theory (DFT) [21,22] as implemented in the Gaussian 03Wquantum chemistry programs [23,24]. Geometry optimization was performed to obtain the stable conformers. Initial calculations were performed using the restricted B3LYP exchange and correlation functional and the 6-311G(d,p) and 6-311++G(d,p) [25,26] basis sets for all atoms. Default SCF and geometry convergence criteria were used and no symmetry constraints were imposed [27], harmonic frequency analysis based on analytical second derivates was used to characterize the optimized geometry as global minimum on the potential energy surface of the title molecule [28].

Geometry optimization of the molecule, molecular energy, ^{1}H-NMR, ^{13}C-NMR and FT-IR spectrum, UV-*Vis* spectrum, Mulliken charges and dipole moments were calculated by using the same method [29-33]. The obtained frequencies were scaled by 0.984 and 0.979 for 6-311G(d,p) and 6-311++G(d,p), respectively [34]. GIAO (Gauge-Independent Atomic Orbital) method was used to determine NMR chemical shift values [35,36]. The obtained NMR frequencies were scaled by 31.99 ppm and 31.97 ppm for H atom and 184.79 ppm and 184.66 ppm for C atom in 6-311G(d,p) and 6-311++G(d,p), respectively [37].

Results and discussion

N-(4-nitrophenyl)-2, 2-dibenzoylacetamide (NPDBA) is description in Scheme S1 (supplementary materials). The title compound was prepared by the reaction of dibenzoyl acetic acid-*N*-carboxy ethyl amide and 4-nitroaniline and obtained in 65 % yield as colorless solid. The experimental data was obtained and compared with calculated values. The observed and calculated values of the title compound were found to be in well-agreement with each other.

Crystal structure description of the compound

The molecular structure and Ortep-3 view of the title compound, $C_{22}H_{16}N_2O_5$, is given in Figure 1a and b. According to crystallographic data for the title compound (Table 1), the title compound belongs to monoclinic crystal system with space group $P12_1/c1$ which have the following dimensions; a=10.023 (2) Å, b=21.587 (5) Å, c=9.401 (2) Å and β =110.29 (3)°. The molecular structure of the compound is not planar with a dihedral angle N1—C7—C8—C16 of -148.1 (3) Å and N1—C7—C8—C9 of 90.9 (4) Å. The N1—C1 and N1—C7 distance has been observed as 1.409 (4) Å and 1.339 (4) Å. Selected optimized and experimental geometries parameters of the title compound in ground state was given in Table 2.

The crystal packing of the title compound is shown in Figure 2. In the crystal structure, molecules are linked together by intermolecular N—H···O and intramolecular C—H···O interactions with symmetry code (i) 2-x, -y, -z; (ii) x, 1/2-y, 1/2+z. This hydrogen bond generates an intramolecular S(6) ring motif through C—H···O. Details of these bonds and interactions are given in Table 3.

Optimized geometries

The optimized structure parameters of the title compound were calculated by DFT–B3LYP levels with the 6-311G(d,p) and 6-311++G(d,p) basis sets. The selected bond lengths, bond angles and torsion angles were compared with the experimental data of the title compound (Table 3). X-ray crystallographic data and molecular calculations of the title compound have not been reported to best of our knowledge. All calculated geometrical parameters are in good agreement with the experimental structural parameters.

In benzene ring, all carbon-carbon bond lengths were calculated in the range of 1.392—1.403 Å for B3LYP and observed in the range of 1.343—1.395 Å for XRD data. In phenyl ring, C—C bond lengths were observed 1.359—1.389 Å and calculated 1.383—1.406 Å in range. N2—O4, N2—O5, C1—N1 and C7—N1 bond distances were observed as 1.191, 1.178, 1.409 and 1.339 Å, respectively. The experimental bond lengths are in agreement with the theoretical values (1.225, 1.225, 1.401, and 1.364 Å, respectively). These data can be comparable with literature data [38].

The bond angles, C7—C8—C16, C7—C8—C9, C8—C9—C10, C8—C16—C17 and C1—N1—C7 , was observed as 109.3°, 107.9°, 120.9°, 118.7° and 127.8°, whereas these values were calculated as and 108.2°, 116.5°, 118.7°, 118.5° and 128.4°, respectively. N1—C7—O3 bond distances in amide group was observed as 125.3°. The bond angles C17–C16–O2, C8–C16–O2, C10–C9–O1 and C8–C9–O1 were observed as 121.8°, 119.5°, 120.8° and 118.3°, this bond angles were calculated as 122.1, 119.4, 120.5 and 120.8, respectively. These values are in agreement with literature data [39].

The torsion angles $\boldsymbol{\tau}_1$ (N1—C7—C8—C16) were observed as 80.4° for theoretically and as -148.1° for experimentally. Furthermore, (N1—C7—C8—C9) was observed as -41.4° and -90.9° for theoretically and experimentally, respectively. The torsion angles $\boldsymbol{\tau}_1$ (O1—C9—C8—C7) and $\boldsymbol{\tau}_1$ (O3—C7—C8—C9) are 33.4° and 141.2° for B3LYP, respectively. These torsion angles are in agreement with the XRD data (12.3° and -88.0°).

Using the root mean square (RMS) error, experimental and theoretical data were compared (Figure3). It was found that the B3LYP/6-311G(d,p) calculation provide the lowest RMSE value of 0.025 Å and 1.738 for bond lengths and bond angles respectively. Consequently the B3LYP calculation with 6-311G(d,p) basis set predicts the best geometry when compared the calculation with 6-311++G(d,p) levels.

(Figure 1)

(Table 2)

(Figure 2)

(Figure 3)

(Table 3)

Vibrational frequency

In order to facilitate assignment of the observed peaks, we have analyzed some bands and compared calculated results with the experimental ones. Experimental FT-IR spectrum of the title compound is given in Figure S1 (supplementary materials). As seen from Table 4, the FT-IR spectra contain some characteristic bands NH, CH, CO and NO groups. The carboxyamide ligand stated the formation of proposed structure by the appearance of new absorption bands at 3281 cm^{-1} (NH), 3070 (sym) and 3104 (asym) cm^{-1} (Ar-CH), 1689, 1675, 1659 cm^{-1} (C=O), 1595-1507 cm^{-1} (C=C), 1448,1409 cm^{-1}(Ph-NO_2). Di substitue and mono substitue phenyl ring were observed at 804 and 666-686 cm^{-1}, respectively. The high frequency region above 3000 cm^{-1} is the characteristic region for identification phenyl C—H stretching vibrations [40]. In the present case, υCH modes of the phenyl rings are observed at 3070 cm^{-1} in the IR spectrum. The region 1700-500 cm^{-1} has very strong and sharp peaks. All the calculated spectra are in good agreement with the experimental data.

(Table 4)

^{1}H NMR (DMSO-d$_6$, δ ppm):

^{1}H NMR (400 MHz, DMSO-d_6): δ, ppm 11.04 (s, 1H, NH), 8,25(d, 2H, *J*=9.2 Hz, B ring C_1-ArH), 7.99 (d, 4H, *J*= 7.6 Hz, A ring C_3-ArH),7.79 (d, 2H, *J*= 9.2 Hz, B ring C_2-ArH), 7.71 (t, 2H, A rings C_1-ArH)**,** 7.59 (t, 4H, A rings C_2-ArH), 6.90 (s, 1H, aliphatic C-H).The ^{1}H-NMR spectra (Figure S2 (supplementary materials)) were in good agreement with the structure of N-(4-nitrophenyl)-2,2-dibenzoylacetamide. In the ^{1}H-NMR spectrum of the compound in DMSO-d_6, the aromatic protons appeared as a broad band at 7.71-8.25 ppm, –NH proton at 11.04 ppm and –CH proton among three carbonyl groups at 6.90 ppm.

^{13}C NMR (DMSO-d_6, δ ppm):

65.00 (aliphatic carbon-$C_{(6)}$); 119.40 (B aromatic ring $C_{(9)}$); 125.60 (B ring $C_{(10)}$); 128.87 (A aromatic rings $C_{(2)}$); 129.57 (A aromatic rings $C_{(3)}$); 134.52 (A aromatic rings $C_{(1)}$); 135.98 (A aromatic rings $C_{(4)}$); 143.09 (B aromatic ring $C_{(11)}$); 145.09 (B aromatic ring $C_{(8)}$); 165.19 (amide carbonyl (C=O) $C_{(7)}$); 192.70 (A aromatic ring benzoyl carbonyls (C=O) $C_{(5)}$). The ^{13}C NMR spectrum of compound is analyzed carbonyl (-C=O) carbon resonance is observed characteristic peaks sequentially at δ 165.19 carbonyl related to amide and 192.70 ppm carbonyl related to benzoyl. In the compound, carbon atoms include one hydrogen in benzene rings located at 119.4, 125.6, 128.87, 129.57, 134.52 and C—H aliphatic carbon (C_6) among three carbonyl carbons at 65.00 ppm (Figure S3 (supplementary materials)). The carbons atom without hydrogen in benzene rings observed at 135.98, 143.09 and 145.09 ppm. Chemical shifts of the peaks of the carbon in the aromatic ring due to the effect substituents are compatible with the literature data [41]. As can be seen from Table 5, the theoretical ^{1}H and ^{13}C chemical shift results for the title compound are generally closer to the experimental ^{1}H and ^{13}C shift data. Both 6-311G(d,p) and 6-311++G(d,p) have showed good conformity.

(Table 5)

Electronic absorption spectra

Ultraviolet spectra analyses of N-(4-nitrophenyl)-2, 2-dibenzoylacetamite) (NPDBA) have been investigated by experimentally and theoretically. The UV-*Vis* spectra of the title compound in ethanol and methanol solvents were recorded within the 190-1100 nm range. The maximum is observed at 320 nm related to n-π^* transition of the amide and benzoyl carbonyl groups (Figure S4 in supplementary materials). In addition, the maximum at 260 nm is related to π-π^* transition of phenyl rings. The calculated frontier orbital energies, absorption wavelength (λ), excitation energies (E) and oscillator strength (*f*) for gas phase and solvent are given in Table 6.

(Table 6)

HOMO and LUMO analysis

The calculations indicate that the compound has 101 occupied molecular orbitals (MOs). The energy gap between HOMO and LUMO of the molecule indicate that this molecule is very stable [42]. Figure 4 shows the distributions and energy levels of the HOMO-1, HOMO, LUMO and LUMO+1 orbitals computed at the B3LYP/6-311++G(d,p) level for the title compound. The positive and negative phase has been seen in red and green color, respectively. The energy gap between the highest occupied and the lowest unoccupied molecular orbitals, is a critical parameter in determining molecular electrical transport properties because it is a measure of electron conductivity.

HOMO energy = -6.9713eV
LUMO energy = -2.7494eV
HOMO-LUMO energy gap = 4.2219eV

The energy values of HOMO and LUMO are computed as -7.0254, -7.0186 and -6.9713 eV; -3.0251, -3.0264 and -2.7494 eV in ethanol, methanol and gas phase, respectively. The energy gap values of the title compound are 4.0003, 3.9922 and 4.2219 eV in ethanol, methanol and gas phase, respectively. According to Koopmans theorem, the values of electronegativity, hardness, softness, electrophilicity index and dipole moment of the molecule were calculated as 5.0252, 2.0001, 0.2499, 6.3128 eV and 13.7011 debye in ethanol, respectively [43-46]. The electronic properties values for the molecules are shown in Table S1 (supplementary materials).

(Figure 4)

Molecular electrostatic potential

Molecular electrostatic potential is related to the electronic density and is a very useful descriptor for determining sites for hydrogen bonding interactions as well as electrophilic attack and nucleophilic reactions [47,48]. The electrostatic potential $V(r)$ at any point in space around a molecule by charge distribution is given by

$$V(r) = \sum Z_A/|R_A-r| - \int \rho(r^l)/|r^l-r|dr^l$$

where the summation runs over all the nuclei *A* in the molecule and polarization and reorganization effect is neglected. Z_A is the charge of the nucleus *A*, located at R_A and $\rho(r^l)$ is the electron density function of the molecule.

The different values of the electrostatic potential at the surface are represented by different colors. The electrostatic potential increases in the order red < orange < yellow < green < blue. The color code of these maps is in the range between -0.02573 a.u. (dark red) and 0.02573 a.u. (dark blue) in compound. The negative (red color) regions of MEP were related to electrophilic reactivity and the positive (blue color) ones to nucleophilic reactivity. As seen from Figure 5, the negative potential regions (red) are over the O atom on the NO2 bonded to aromatic ring, amide carbonyl (C=O) and aromatic tile carbonyl (C=O) group. The positive potential regions (blue) are over the H atom on the aliphatic (C-H) and aromatic tiles. Considering these calculated results, the MEP map shows that the negative potential sites are on electronegative O atoms as well as the positive potential sites are around the hydrogen atoms, respectively.

(Figure 5)

Mulliken population analysis and natural population analysis

The calculated Mulliken atomic charges and natural population analysis (NPA) atomic charges of N-(4-nitrophenyl)-2, 2-dibenzoylacetamite) (NPDBA) are presented in Table S2 (supplementary materials). The Mulliken population analysis and NPA are obtained from optimized geometry and NBO [49] results, respectively. In all these compound among the C17 atom has the highest positive charge (0.917 e^-) due to highly electronegative Oxygen atoms (O1 = -0.571 e^- and O3 = -0.614 e^-) present in the adjacent position. The charge of the O3 (-0.614 e^-) atom is the highest negative value at NPA. However, charge value for O4 and O5 (-0.007 e^-) atoms at Mulliken population analysis are nearly neutral. As can be seen in Table S2 (supplementary materials), all the hydrogen atoms have a net positive charge and all the oxygen atoms have a net negative charge. Natural Population Analysis shows that the H1 atom has maximum positive atomic charges (0.449 e^-; 0.435 e^-) than the other hydrogen atoms. The total dipole moments were obtained as 10.88 and 10.88 Debye by using Mulliken population analysis and NPA, respectively.

Natural bond orbital analysis (NBO)

Natural bond orbital (NBO) analysis is a helpful tool for understanding the bond-antibond stabilization energies within the title compound, interaction among bonds, and charge transfer or conjugative interaction in molecular systems [50-53]. The Natural Bond Orbital (NBO) calculations were performed via NBO 3.1 program [54] as implemented in the Gaussian 03W package at the DFT-B3LYP/6-311++G(d,p) level. The second order perturbation approach is used to evaluate the donor (i) and acceptor (j) interaction in the NBO basis [55].

In our study, this system shows some contribution to the π electron delocalization corresponds to the donor–acceptor interactions which are π(C23—C32) →π*(O1—C22) (20.37 kcal/mol), π*(C24—C26) (19.30 kcal/mol), π*(C28—C30) (17.84 kcal/mol); π(C24—C26) →π*(C23—C32) (19.08 kcal/mol), π*(C28—C30) (21.74); π(C28—C30) →π*(C23—C32) (22.88 kcal/mol), π*(C24—C26) (17.36); π(C35—C44) →π*(O2—C34) (19.31 kcal/mol), π*(C36—C38) (19.78 kcal/mol), π*(C40—C42) (17.74 kcal/mol); π(C36—C38) →π*(C35—C44) (18.83 kcal/mol), π*(C40—C42) (21.62 kcal/mol); π(C40—C42) →π*(C35—C44) (22.82 kcal/mol), π*(C36—C38) (17.61 kcal/mol), while π(C9—C10) →π*(C12—C14) (25.31 kcal/mol), π*(C15—C17) (16.34 kcal/mol); π(C12—C14) →π*(O5—N8) (26.43 kcal/mol), π*(C9—C10) (16.61 kcal/mol), π*(C15—C17) (22.01 kcal/mol); π(C15—C17) →π*(C9—C10) (21.51 kcal/mol), π*(C12—C14) (17.30 kcal/mol) for the phenyl rings of the molecule. The most important interaction energies are LP(1)N6 →π*(O3—C19) (63.22 kcal/mol) and π*(C9—C10) (38.06 kcal/mol); LP(3)O4→π*(O5—N8) (160.60 kcal/mol). Finally, n(O1—C22), n(O2—C34), n(O5—N8) lead to an enormous stabilization of 120.69, 128.68 and 17.57 kcal/mol, respectively. This strong stabilization denotes the larger delocalization. This highest interaction around the ring can induce the large bioactivity in the compound [50]. The hyper conjugative interaction and electron density transfer from lone electron pair of the O1 atom to the N6—H7 anti bonding orbital in the N6—H7···O1 system, O3 atom to C10—H11 and C44—H45 anti bonding orbital in C10—H11···O3 and C44—H45···O3 have been predicted. This hydrogen bonding is formed by the orbital overlap between LP(2)O1 → BD*(1) N6—H7 (6.87 kcal/mol), LP(1) O3 → BD*(1) C10—H11 (0.53 kcal/mol), LP(2) O3→BD*(1) C10—H11 (1.10 kcal/mol) and LP (2) O3→BD*(1) C44—H45(0.61 kcal/mol) which consequences inter and intra molecular charge transfer (ICT) causing stabilization of the hydrogen bonded system. The results for title compound were presented in Table S3 (supplementary materials).

Nonlinear optical effects (NLO)

The polar properties of the title compound were calculated at the DFT-B3LYP/6-311++G(d,p) level using Gaussian 03W program package. Urea is one of the prototypical molecules used in the study of the Non Linear Optical (NLO) properties of molecular system. As can be seen in Table S4 (supplementary materials), calculated values of μ_{tot}, α_{tot} and β_{tot} for the title compound are, 4.281 debye, 45.800 $Å^3$ and $2.283x10^{-29}cm^5/esu$ and the title molecule is 61.2 times greater than those of urea (μ_{tot} and β_{tot} of urea are 1.3732 debye and $0.3728x10^{-30}cm^5/esu$, respectively [50]. According to these results, the title compound is a good candidate of NLO material.

Conclusion

N-(4-nitrophenyl)-2, 2-dibenzoylacetamite) (NPDBA), $C_{22}H_{16}N_2O_5$, was synthesized and characterized by experimental (X-Ray, FT-IR, NMR and UV-*Vis*) and by theoretical methods in DFT-B3LYP/6-311G(d,p) and B3LYP/6-311++G(d,p) levels. The crystal structure of the title compound is stabilized by the C—H···O and N—H··O type hydrogen bonds. In order to understand electronic transitions of compound, TD-DFT calculations on electronic absorption spectra in gas phase and solvent (ethanol and methanol) were performed. Theoretical calculations of ^{13}C and ^{1}H-NMR chemical shifts, FT-IR frequencies and geometrical parameters contribute to a better understanding of the experimental spectra. The MEP map shows that the negative potential sites are on electronegative O atoms as well as the positive potential sites are around the hydrogen atoms. Frontier molecular orbital energies and molecular electronic potential are calculated using B3LYP/6-311G(d,p) and 6-311++G(d,p) level, and obtained small HOMO–LUMO energies show that charge transfer occurs in the title compound. Electronic transition of the title compound has observed good chemical stability with 4.24 eV value. Mulliken population analysis and natural population analysis have showed maximum positive atomic charges around the C17 (Mulliken charges) atom. All the hydrogen atoms have a net positive charge. Natural Population Analysis shows that the H1 atom has maximum positive atomic charges than the other hydrogen atoms. Nonlinear optical properties of the title compound were found greater than those of urea. Natural bond orbital (NBO) calculations reveals N6—H7···O1 and C10—H11···O3 hyper-conjugation interaction.

Supplementary data

Crystallographic data for the structure reported in this article was deposited with the Cambridge Crystallographic Data Centre as supplementary publication number CCDC 1042436. Copies of the data can be obtained free of charge on application to CCDC 12 Union Road, Cambridge CB21 EZ, UK.
(Fax: (+44) 1223 336-033; e-mail: data_request@ccdc.cam.ac.uk).

Acknowledgment

This study was funded from Presidency of Scientific Research Projects of University Gaziantep (FEF.10.08). The authors thank Harran University Chemistry Department and Central Laboratory for IR and NMR, respectively; Dokuz Eylül University for XRD measurement of the title compound.

References

[1] A. Balaban, N.Çolak, H. Ünver, B. Erk, T.N. Durulu, and M.D. Zengin, J. Chem.Cryst., 38 (2008), 369-372.

[2] D.N. Lee, J.Y. Ryu, H. Kwak, Y.M. Lee, S.H. Lee, J.T. Poong, J. Lee, W. Shin, C. Kim, S-J. Kim, Y. Kim,J. Mol.Struct., 885 (2008), 56-63.

[3] V. Ravinder, S.J. Swamy, S. SriHari,P. Lingaiah, Polyhedron, 4 (1985), 1511.

[4] R. Drago, S.A. Wentz, R.L. Carlson, J. Am. Chem. Soc., 84 (1962), 1106.

[5]E. Ziegler, G. Kollenz, W. Ott, Communications Synthesis. (1973) 679-680.

[6]I. Yıldırım, I.I. Ozer, J. HeterocyclicChem. 34 (1997) 1047-1051.

[7]I.Yıldırım, İ.Ö. İlhan, Indian J.Chem.Sect. B 36 (1997) 1138-1147.

[8] W.F. Fabian, G. Kollenz, Y. Akcamur, T.R. Kok, M. Tezcan, M. Akkurt und W. Hiller, Monath. Chem.,123 (1992) 265.

[9] H. Tanak, A.A. Ağar, O. Büyükgüngör, Spectrochim.Acta Part A 118 (2014) 672–682.

[10] E.İnkaya, M.Dinçer, E.Sahan, I.Yıldırım, Spectrochim.Acta Part A 114 (2013) 92–100.

[11] A.D. Becke, J. Chem. Phys. 98 (1993) 5648–5652.

[12] H. Tanak, Molecular Physics, 112 (2014) 1553-1565.

[13] C. Lee, W. Yang, R.G. Parr, Phys. Rev. B 37 (1988) 785–789.

[14] Ü. Ceylan, M.E. Hacıyusufoğlu, M. Sönmez, Ş.P. Yalçın, N. Özdemir, Spectrochim. Acta Part A 141 (2015) 307-315.

[15] K. Sarojini, H. Krishnan, Charles C. Kanakam, S. Muthu, Spectrochim.Acta Part A 108 (2013) 159–170

[16] Agilent (2012). CrysAlis PRO.Agilent Technologies, Yarnton, Oxfordshire, England.

[17] J. O. Morley, T. P. Matthews, Org. Biomol. Chem,,4 (2006) 359-366.

[18] L.J. Farrugia, J. Appl. Cryst., 30 (1997) 565.

[19] L. J. Farrugia, J. Appl. Cryst.32(1999) 837-838.

[20] G. M. Sheldrick, ActaCryst. A64(2008) 112-122.

[21] C. Lee, W. Yang and R. G. Parr, Phys. Rev. B37 (1988)785.

[22] A. D. Becke, J. Chem. Phys. 98 (1993) 5648.

[23] R. Dennington II, T. Keith, J. Millam, Gaussview, version 4.1.2, Semichem, Inc. Shawnee Mission, KS, (2007).

[24] M,J, Frisch, G,W, Trucks, H,B, Schlegel, G,E, Scuseria, M,A, Robb, J,R, Cheeseman, J,A, Montgomery, Jr,, T, Vreven, K,N, Kudin, J,C, Burant, J,M, Millam, S,S, Iyengar, J, Tomasi, V, Barone, B, Mennucci, M, Cossi, G, Scalmani, N, Rega, G,A, Petersson, H, Nakatsuji, M, Hada, M, Ehara, K, Toyota, R, Fukuda, J, Hasegawa,M, Ishida, T, Nakajima, Y, Honda, O, Kitao, H, Nakai, M, Klene, X, Li, J,E, Knox, H,P, Hratchian, J,B, Cross, C, Adamo, J, Jaramillo, R, Gomperts, R,E, Stratmann, O, Yazyev, A,J, Austin, R, Cammi, C, Pomelli, J,W, Ochterski, P,Y, Ayala, K, Morokuma, G,A, Voth, P, Salvador, J,J, Dannenberg, V,G, Zakrzewski, S, Dapprich, A,D, Daniels, M,C, Strain, O, Farkas, D,K, Malick, A,D, Rabuck, K, Raghavachari, J,B, Foresman, J,V, Ortiz, Q, Cui, A,G, Baboul, S, Clifford, J, Cioslowski, B,B, Stefanov, G, Liu, A, Liashenko, P, Piskorz, I, Komaromi, R,L, Martin, D,J, Fox, T, Keith, M,A, Al- Laham, C,Y, Peng, A, Nanayakkara, M, Challacombe, P,M,W, Gill, B, Johnson, W, Chen, M,W, Wong, C, Gonzalez, J,A, Pople, GAUSSIAN 03, Revision B,05, Gaussian, Inc,, Pittsburgh, PA, (2003).

[25] A. Frisch, A.B. Nielsen, A.J. Holder, Gaussview User Manual, Gaussian Inc., Pittsburg (2001).

[26] R. Ditchfield, W.J. Hehre and J.A. Pople, J. Chem. Phys., 54 (1971) 724-718.

[27] A. Wagner, R. Flaig, D. Zobel, B. Dittrich, P. Bombicz, M. Strümpel, and P. Luger, J. Phys. Chem. A 106 (2002) 6581-6590.

[28]J. M. Bowman, B. J. Braams, S. Carter, C. Chen, G. Czako, B. Fu, X. Huang, E. Kamarchik, A. R. Sharma, B. C. Shepler, Y. Wang, and Z. Xie, J. Phys. Chem. Lett., 1 (2010) 1866–1874.

[29] G. Fitzgerald, J. Andzelm, J. Phys. Chem., 95 (1991) 10531-10534.

[30] Ü. Ceylan, M. Durgun, H. Türkmen, Ş.P. Yalçın, A. Kılıç, N. Özdemir, J. Mol. Struct. 1089 (2015) 22-232.

[31] S. Bayarı, S. Sağlam, H. F. Üstündağ, J. Mol. Struc., 726 (2005) 225-232.

[32] Z. Dega-Szafran, A. Katrusiak, M. Szafrn, J. Mol. Struc., 741 (2005) 1-9.

[33] A. A. Ağar, H. Tanak, M. Yavuz, Mol. Phys., 108 (2010) 1759-1772.

[34] F. Kandemirli, Y. Akkaya, C.D. Vurdu, Asian Journal Chem. 25, 9722-9730 (2013) 32-33

[35] J. L. Dodds, R. McWeeny, A. J. Sadlej, Mol. Phys., 34 (1977) 1779-1791.

[36] K. Wolinski, J. F. Hinton, P. Pulay, J. Am. Chem. Soc., 112 (1990) 8251-8260.

[37] E. İnkaya, M. Dinçer, E. Şahan, I. Yıldırım, Spectrochim. Acta Part A114 (2013) 92-100.

[38] R.M. Fuquen, Al. Azcarate, A.R. Kennedy, D. Gilmour and R.H.D.A. Santos, ActaCryst., (2013) E69, o1592.

[39] T.Yeşilkaynak, G.Binzet, F. M.Emen, U.Flörke, N.Külcü and H.Arslan, European Journal of Chemistry, 1 (1) (2010) 1-5.

[40] Z.R. Zhou and Z.X. Zhou, Indian Journal of Pure applied Physics, 51, 164-173, 2013.

[41] H. Masu, T. Okamoto, T. Kato, K.Katagari, M.Tominaga, H.Goda, H.Takayanagi, I.Azumaya, Tetrahedron Letters. 47 (2006), 803-807.

[42] K. Kuki, Science 218 (1982) 747-754.

[43] Z.Demircioğlu, Ç.Albayrak, O. Büyükgüngör, J. Mol. Struct. 1055-1066(2014), 210-222.

[44] N. Özdemir, S. Dayan, O. Dayan, M. Dinçer, N.Ö. Kalaycıoğlu, Mol. Phys. (2012) 1-17.

[45] H. Tanak, A. A. Ağar, O. Büyükgüngör, J. Mol. Struct. 1048 (2013) 41-50.

[46] H. Pir, N. Günay, D. Avcı, Y. Atalay, Spectrochim. Acta A 96 (2012) 916-924.

[47] E. Scrocco, J. Tomossi, Adv. Quant. Chem. 11(1978)115-121.

[48] F.J. Luque, J.M. Lopez, M. Orozco, Theor. Chem. Acc. 103(2000) 343-345.

[49] R.S. Mulliken, J. Chem. Phys. 23 (1955) 1833-1840.

[50] K. Govindarasu, E. Kavitha, N. Sundaraganesan, Spectrochim.Acta Part A 133 (2014) 417–431.

[51] M. Snehalatha, C. Ravikumar, I. Hubert Joe, N. Sekar, V.S. Jayakumar, Spectrochim. Acta A 72 (2009) 654–662.

[52] H. Tanak, A.A. Ağar, O. Büyükgüngör, Spectrochim. Acta Part A 118 (2014) 672–682.

[53] H. Tanak, Mariusz K. Marchewka, J.Mol.Struct. 1034 (2013) 363–373

[54] E.D. Glendening, A.E. Reed, J.E. Carpenter, F. Weinhold, NBO Version3.1, TCI, University of Wisconsin, Madison, 1998.

[55] A.E. Reed, L.A.F. Curtiss, Chem. Rev. 88 (1988) 899–926.

Figure Captions:

Figure 1 (a) Ortep 3 diagram of the title compound with the atom numbering scheme. Displacement ellipsoids were drawn at the 50% probability. Dashed lines are show the C–H···O intramolecular hydrogen bonds. (b) The theoretical geometric structure of the title compound (B3LYP/6-311++G(d,p) level).

Figure 2 Packing diagram of the title compound along the b axis.

Figure 3 Atom-by-atom superimposition of the structures calculated (red) [a= B3LYP/6-311G(d,p) and b= B3LYP/6-311++G(d,p)] over the X-ray structure (black) for the title compound. Hydrogen atoms omitted for clarity.

Figure 4 The atomic orbital compositions of the frontier molecular orbital for N-(4-nitrophenyl)-2, 2-dibenzoylacetamite) (NPDBA).

Figure 5 Molecular electrostatic potential map calculated as the B3LYP/6-311++G(d,p) level.

Table 1 Crystallographic data for the title compound.

Formula Sum	$C_{22}H_{16}N_2O_5$
Crystal System	Monoclinic
Space Group	'P121/c1'
Formula weight	388.37
λ(Å)	0.71073
Temperature (^{0}K)	293(2)
Volume(Å^3)	1907.8 (7)
Z	4
a, b, c (Å)	10.023(2),21.587(5),9.401(2)
β(^{0})	110.29(3)
Calculated density (Mg/m^3)	1.352
μ (mm^{-1})	0.097
F(000)	808.0
Crystal size (mm)	0.5241 × 0.2252 × 0.1561
θ range for data collection(^{0})	5.96-52.72
Refinement method	Full-matrixleast-squares on F^2
Absorption correction	analytical
Limiting indices	$-10 \leq h \leq 12$, $-26 \leq k \leq 17$, $-11 \leq l \leq 11$
Measured reflections	8061
Independent reflections	3900
Goodness -of-fit on F^2	1.002
Weighting scheme	$w = 1/[\sigma^2(F_o^2) + (0.1548P)^2 + 0.0000P]$; $P = (F_o^2 + 2F_c^2)/3$
R_{int}	0.1027
$R[F^2>2\sigma(F^2)]$, $wR(F^2)$	0.0972, 0.3037
Largest diff. Peak and hole (e Å^{-3})	0.51and -0.58

Table 2 Selected optimized and experimental geometries parameters of the title compound in ground state.

Parameters	**Experimental**	**Calculated (B3LYP)**	
		6-311G(d,p)	**6-311++G(d,p)**
Bond lengths (Å)			
O1—C9	1.217 (5)	1.218	1.219
O2—C16	1.207 (5)	1.210	1.211
C8—C16	1.523 (5)	1.562	1.563
C9—C10	1.464 (5)	1.492	1.492
O3—C7	1.209 (4)	1.218	1.219
C10—C11	1.378 (6)	1.403	1.404
O4—N2	1.191 (6)	1.225	1.227
C10—C15	1.393 (6)	1.401	1.402
O5—N2	1.178 (6)	1.225	1.226
C11—C12	1.377 (7)	1.387	1.387
N1—C1	1.409 (4)	1.401	1.401
C12—C13	1.359 (9)	1.395	1.396
N1—C7	1.339 (4)	1.364	1.363
C13—C14	1.355 (9)	1.392	1.393
N2—C4	1.472 (6)	1.471	1.470
C14—C15	1.353 (7)	1.391	1.392
C1—C2	1.375 (5)	1.404	1.404
C16—C17	1.477 (5)	1.492	1.492
C1—C6	1.376 (5)	1.406	1.406
C17—C18	1.395 (6)	1.403	1.404
C2—C3	1.389 (6)	1.388	1.389
C17—C22	1.380 (6)	1.401	1.402
C3—C4	1.373 (6)	1.390	1.391
C18—C19	1.380 (7)	1.387	1.388
C4—C5	1.359(6)	1.392	1.393
C19—C20	1.343 (7)	1.396	1.396
C5—C6	1.371 (6)	1.383	1.383
C20—C21	1.363 (7)	1.393	1.393
C7—C8	1.535 (5)	1.547	1.548
C21—C22	1.381 (6)	1.392	1.392
C8—C9	1.524 (5)	1.532	1.533
RMSE[*]		0.025	0.026
Max. Difference[*]		0.008	0.008
Bond Angles (°)			
C7—N1—C1	127.8 (3)	128.4	128.5
O1—C9—C10	120.8 (4)	120.5	120.6
O4—N2—C4	118.1 (5)	117.7	117.8
C10—C9—C8	120.9 (3)	118.7	118.6
O5—N2—O4	123.1 (5)	124.6	124.4
C11—C10—C9	118.3 (4)	117.4	117.5
O5—N2—C4	118.7 (5)	117.7	117.8
C2—C1—N1	123.5 (3)	123.5	123.6
C15—C10—C9	122.7 (4)	123.5	123.4
C2—C1—C6	119.9 (4)	119.6	119.6

C12—C11—C10	119.8 (5)	120.5	120.5
C6—C1—N1	116.6 (3)	116.8	116.7
C13—C12—C11	119.9(5)	120.0	120.0
C1—C2—C3	119.5(4)	119.6	119.6
C14—C13—C12	120.6 (5)	120.0	120.0
C4—C3—C2	119.0 (4)	119.8	119.8
C15—C14—C13	120.7 (6)	120.1	120.1
C3—C4—N2	118.5(4)	119.4	119.4
C14—C15—C10	120.0 (5)	120.3	120.3
C5—C4—N2	119.6 (5)	119.2	119.2
O2—C16—C8	119.5(4)	119.4	119.4
C5—C4—C3	122.0 (4)	121.3	121.3
O2—C16—C17	121.8 (4)	122.1	122.1
C17—C16—C8	118.7 (3)	118.5	118.5
C18—C17—C16	118.9 (4)	117.4	117.5
O3—C7—N1	125.3 (3)	125.7	125.6
C22—C17—C16	122.8 (4)	123.1	123.0
O3—C7—C8	120.8 (3)	119.2	119.1
N1—C7—C8	113.8 (3)	114.9	115.2
C19—C18—C17	119.6 (5)	120.2	120.2
C9—C8—C7	107.9 (3)	116.5	116.7
C20—C19—C18	121.4 (3)	119.9	119.9
C16—C8—C7	109.3 (3)	108.2	108.3
C19—C20—C21	120.0 (5)	120.1	120.0
C16—C8—C9	111.2 (3)	108.0	108.1
C20—C21—C22	120.1 (5)	120.2	120.1
O1—C9—C8	118.3 (3)	120.8	120.8
C17—C22—C21	120.6 (4)	119.9	119.9
RMSE*		1.738	1.758
Max. Difference*		3.200	3.100
Torsion Angles (º)			
O1—C9—C10—C11	7.8 (6)	-4.7	-4.8
O1—C9—C10—C15	-169.5 (4)	174.1	174.0
O2—C16—C17—C18	-7.2 (6)	-14.7	-15.5
O2—C16—C17—C22	171.8 (4)	163.6	162.8
O3—C7—C8—C9	-88.0 (4)	141.2	141.8
O3—C7—C8—C16	33.0 (5)	-96.8	-95.8
O4—N2—C4—C3	-175.9 (6)	-179.9	-179.9
O4—N2—C4—C5	3.2 (9)	0.1	0.1
O5—N2—C4—C3	7.1 (8)	0.1	0.1
O5—N2—C4—C5	-173.8 (6)	-179.9	-179.9
N1—C1—C2—C3	-179.4 (4)	179.3	179.3
N1—C1—C6—C5	-179.9 (4)	-179.4	-179.4
N1—C7—C8—C9	90.9 (4)	-41.4	-40.7
N1—C7—C8—C16	-148.1 (3)	80.4	81.4
N2—C4—C5—C6	-179.0 (5)	179.9	179.9
C9—C8—C16—O2	14.6 (5)	38.1	39.9

*****RMSE and maximum differences between the bond lenghts and angles computed using theoretical method and those obtained from X-ray diffraction.

Table 3 Hydrogen bond geometry (Å, º)

D—H···A	D—H(Å)	H···A(Å)	D···A(Å)	D—H···A(º)
C2—H2···O3	0.93	2.28	2.8671	120
C3—H3···O5^{i}	0.93	2.45	3.3603	165
C6—H6···O1^{ii}	0.93	2.42	3.2032	142
C8—H8···O3^{ii}	0.98	2.46	3.1585	128
N1—H1···O3^{ii}	0.86	2.13	2.9459	159

Note: Symmetry codes: (i) 2-x, -y,- z; (ii) x, 1/2-y, 1/2+z.

Table 4 Comparison of the experimental and calculated vibrational frequencies (cm^{-1}).

Assignment*	**Experimental**	**Calculated (B3LYP)**	
		6-311G(d,p)	**6-311++G(d,p)**
$\nu(\text{N-H})_{\text{aliphatic}}$	3281	3397	3376
ν(C-H)	3104	3139	3135
ν(C-H)	3070	3128	3122
$\nu(\text{C=O})_{\text{benzoyl}}$	1689	1735	1717
ν(C=O) + ν(N-H)	1675	1728	1707
ν(C=O)	1659	1695	1675
γ(N-H)	1618	1629	1616
$\gamma(\text{C=C})_{\text{as}}$	1595	1616	1603
$\nu(\text{NO}_2)_{\text{as}}$ + γ(N-H)	-	1585	1566
$\nu(\text{NO}_2)_{\text{as}}$ + γ(N-H)	1448	1550	1550
$\gamma(\text{C-H})_{\text{s}}$	-	1503	1494
$\gamma(\text{C-H})_{\text{benzoyl}}$	-	1456	1446
α(C-H)	-	1422	1412
$\nu(\text{NO}_2)_{\text{as}}$ + γ(N-H)	1409	1354	1328
β(ring)	1334	1338	1328
γ(C-H)	1284	1252	1298
γ(C-H)	1239	1226	1217
$\omega(\text{C-H})_{\text{phenyl}}$	804	800	792
$\omega(\text{C-H})_{\text{phenyl}}$	751	770	762
γ(N-H)	686	716	712
ω(C-H)	679	696	687

* ν: Stretching, s: Symmetric, γ: rocking, ω: wagging, α: scissoring

Table 5 Theoretical and experimental ^{1}H-NMR and^{13}C-NMRchemical shift (with respect to TMS, all values ppm) for the title compound.

Atom	**Experimental (ppm)** **(DMSO-d_6)**	**Calculated (ppm)** **6-311G(d,p)**	**6-311++G(d,p)**
^{1}H-NMR			
H1	11.04	10.63	10.97
H2	7.79	8.95	9.04
H3	8.25	8.39	8.39
H5	8.25	8.41	8.53
H6	7.79	7.17	7.30
H8	6.90	6.69	6.86
H11	7.99	8.73	8.72
H12	7.59	7.73	7.76
H13	7.71	7.73	7.81
H14	7.59	7.45	7.41
H15	7.99	7.81	7.81
H18	7.99	8.33	8.58
H19	7.59	7.66	7.60
H20	7.71	7.81	7.83
H21	7.59	7.83	7.92
H22	7.99	9.18	9.27
^{13}C-NMR			
C1	145.09	151.21	152.45
C2	119.40	123.28	124.57
C3	125.60	131.71	133.36
C4	143.09	151.80	152.12
C5	125.60	130.66	131.91
C6	119.40	122.71	123.28
C7	165.19	165.93	167.33
C8	65.00	70.13	71.08
C9	192.70	197.31	199.20
C10	135.98	141.64	142.30
C11	129.57	136.81	138.33
C12	128.87	135.22	136.05
C13	134.52	141.18	142.30
C14	128.87	134.21	135.27
C15	129.57	134.97	135.79
C16	192.70	192.04	193.91
C17	135.98	142.34	143.42
C18	129.57	137.17	139.09
C19	128.87	134.57	134.95
C20	134.52	140.68	141.75
C21	128.87	134.70	135.88
C22	129.57	138.15	139.51

Table 6 Calculated energies values, chemical hardness, electronegativity, chemical potential, electrophilicity index of N-(4-nitrophenyl)-2,2-dibenzoylacetamite) (NPDBA) UV-vis region.

TD-DFT/B3LYP 6-311++G(d,p)	**Gas Phase (ε=1)**	**Ethanol (ε=24.3)**	**Methanol (ε=32.63)**
E_{total} (Hartree)	-1333.8911	-1333.9197	-1333.9208
E_{HOMO} (eV)	-6.9713	-7.0254	-7.0186
E_{LUMO} (eV)	-2.7494	-3.0251	-3.0264
$\Delta E_{HOMO-LUMO}$	4.2219	4.0003	3.9922
Chemical hardness (η)	2.1109	2.0001	1.9961
Chemical softness (*S*)	0.2368	0.2499	0.2504
Electronegativity (χ)	4.8603	5.0252	5.0225
Chemical potential (μ)	-4.8603	-5.0252	-5.0225
Electrophilicity index (φ)	5.5953	6.3128	6.3186
Dipole moment (Debye)	10.8806	13.7011	13.7599

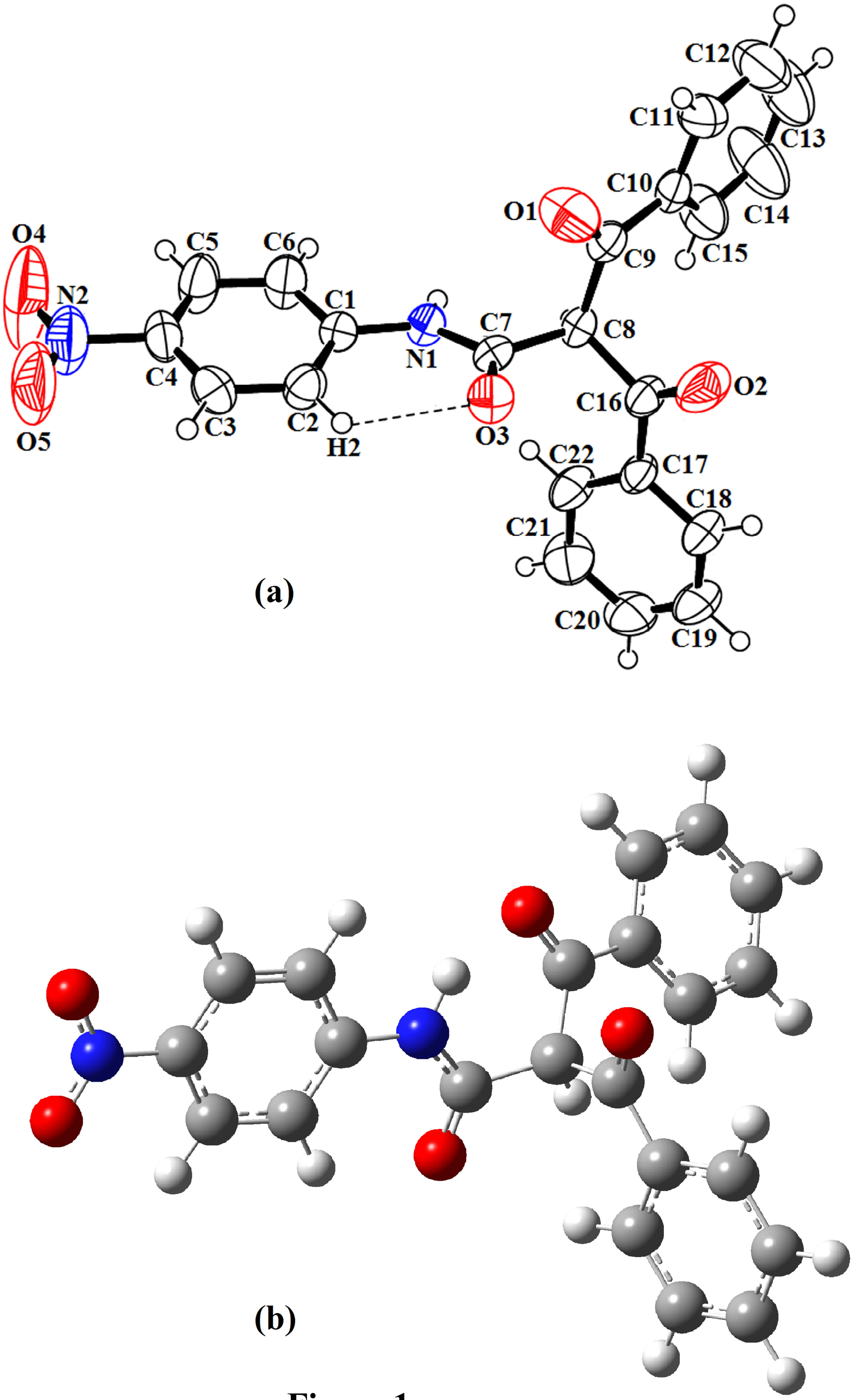
O4
N2
O5
C4
C5
C6
C3
C2
H2
C1
N1
C7
O3
C8
C9
O1
C10
C11
C12
C13
C14
C15
C16
O2
C17
C18
C19
C20
C21
C22

(a)

(b)

Figure 1

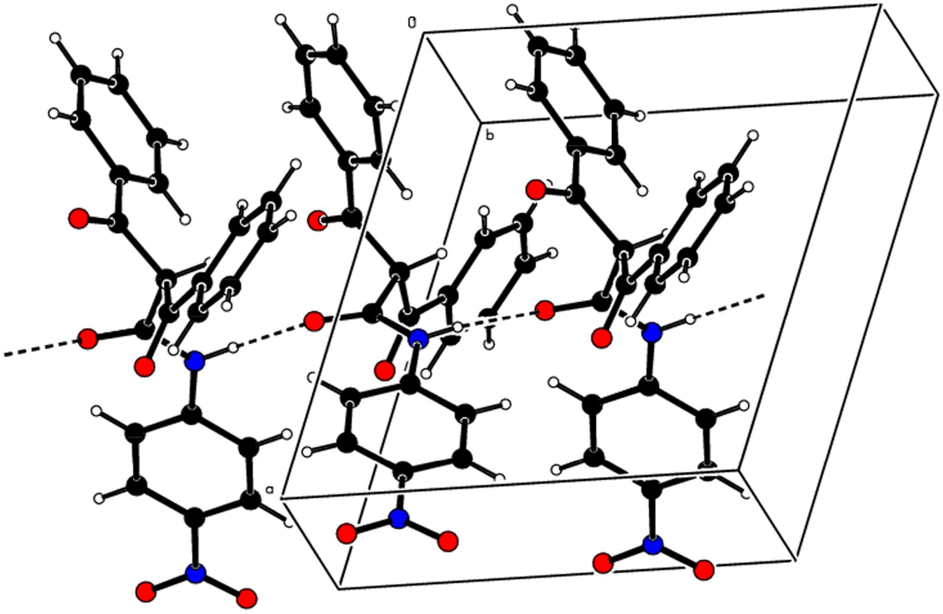

Figure 2

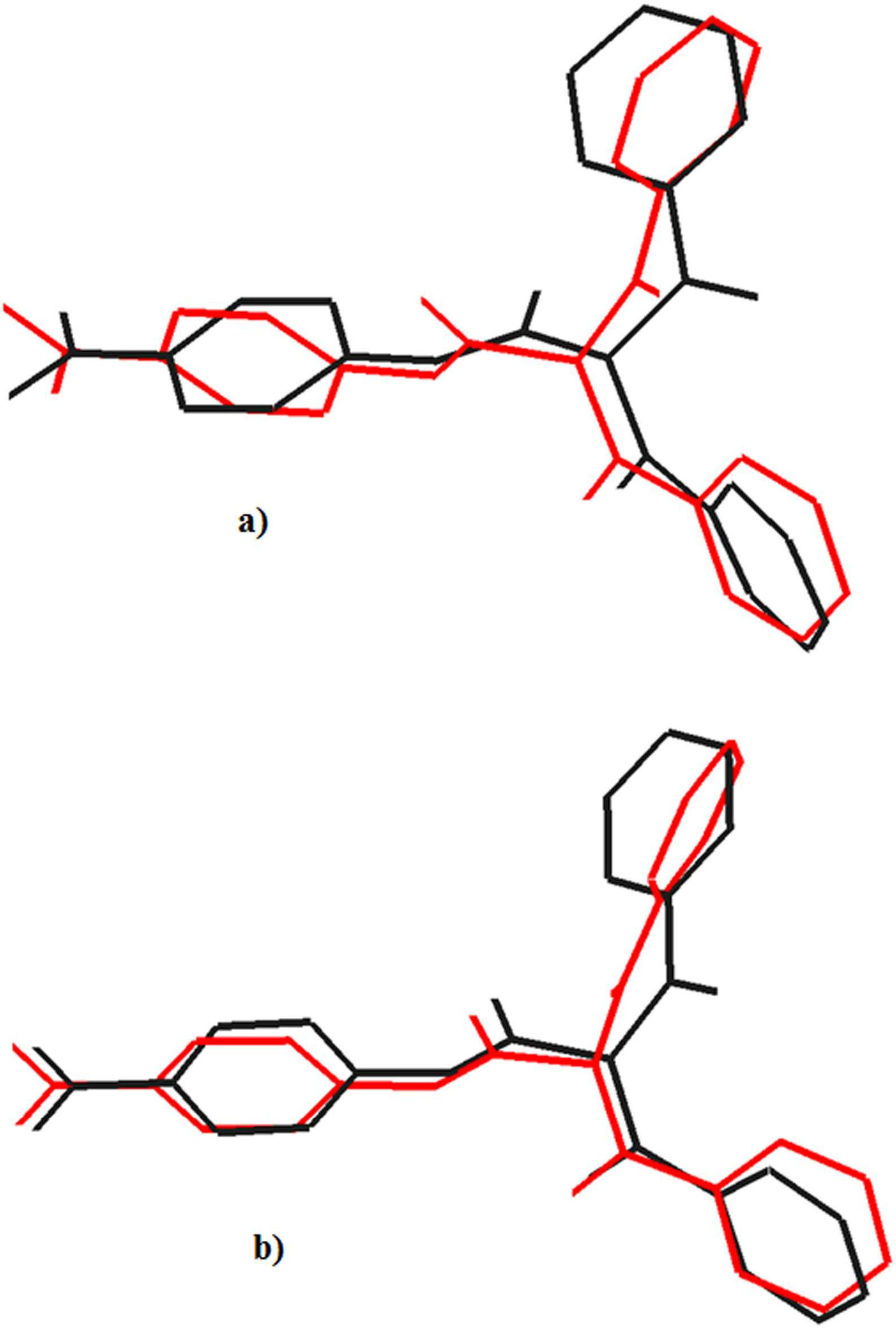

Figure 3

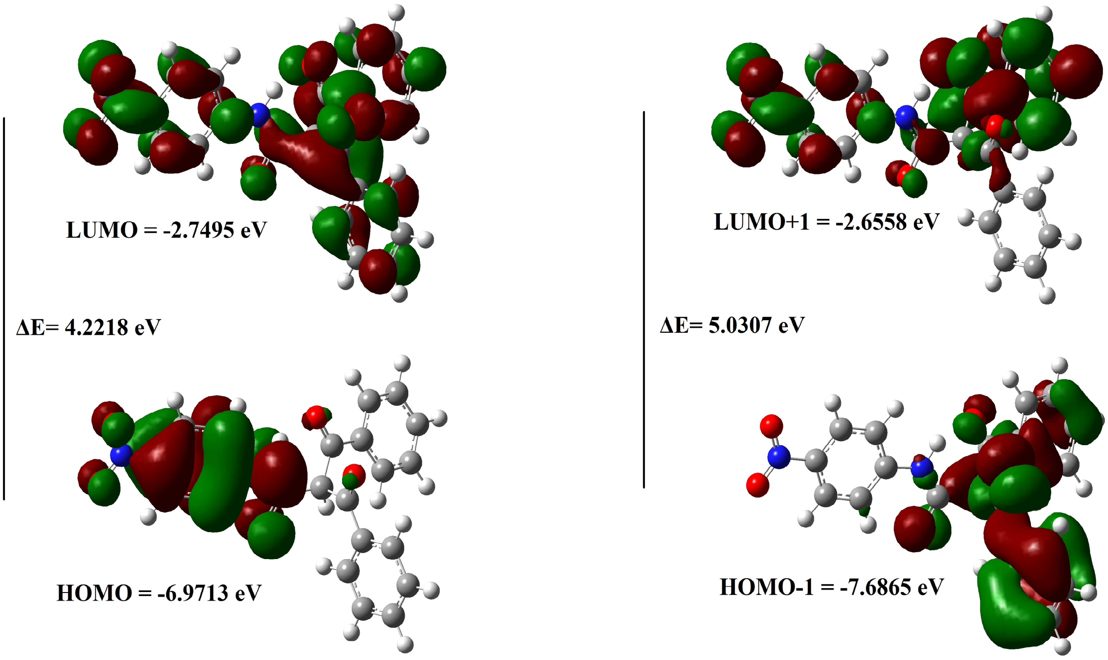
LUMO = -2.7495 eV
ΔE= 4.2218 eV
HOMO = -6.9713 eV
LUMO+1 = -2.6558 eV
ΔE= 5.0307 eV
HOMO-1 = -7.6865 eV

Figure 4

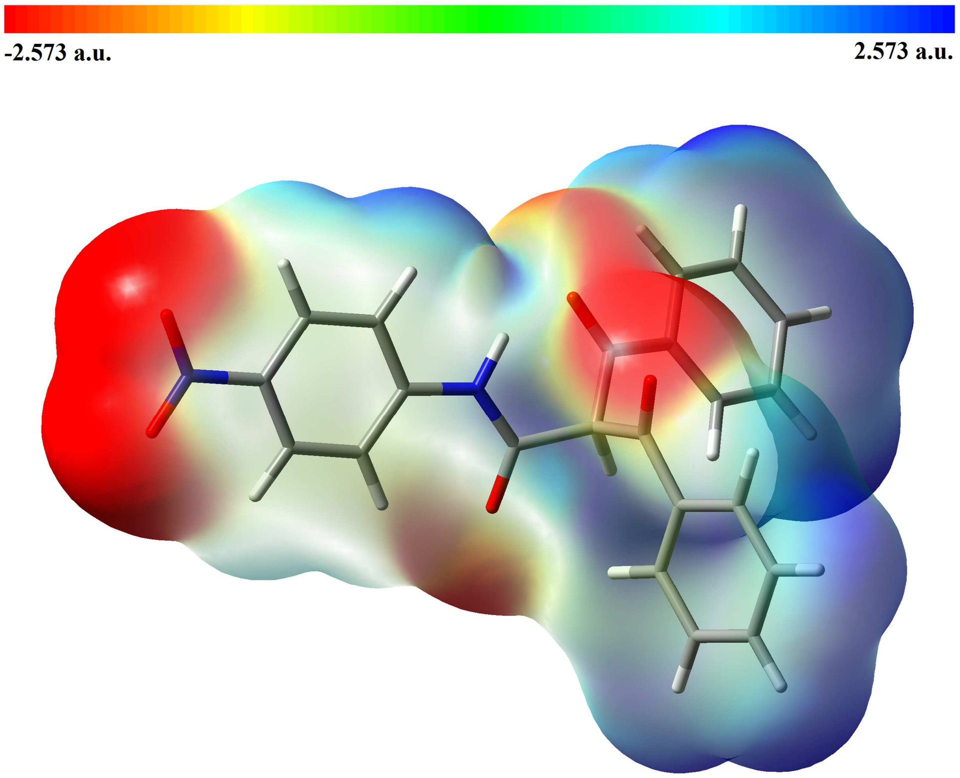

Figure 5

Highlights of paper

- The vibrational frequencies of the compound have been calculated by B3LYP/6-311G(d,p) and B3LYP/6-311++G(d,p) methods.

- NLO and NBO analysis of the molecule were studied.

- HOMO and LUMO energies, absorption wavelength and excitation energies were calculated.

Synthesis, structural, spectral (FT-IR, ^{1}H and ^{13}C-NMR and UV-*Vis*), NBO and first order hyperpolarizability analysis of N-(4-nitrophenyl)-2, 2-dibenzoylacetamide by density functional theory

Şerife Pınar Yalçın[a], Ümit Ceylan[b]✉, Ahmet Oral Sarıoğlu[c],
Mehmet Sönmez[c], Muhittin Aygün[d]

[a]*Central Laboratory, Osmanbey Campus, Harran University, 63190 Şanlıurfa, TURKEY*
[b]*Department of Medical Services and Techniques, Vocational High School of Health Services, Giresun University, 28100 Giresun, TURKEY*
[c]*Department of Chemistry, Faculty of arts and Sciences, Gaziantep University, 27310, Gaziantep, TURKEY*
[d]*Department of Physics, Faculty of arts and Sciences, Dokuz Eylül University,Buca,35150, Izmir, TURKEY*

✉**Corresponding author Tel.:** +90 505 313 51 57

E-mail: umit.ceylan@giresun.edu.tr (Ü. Ceylan); msonmez@gantep.edu.tr, (M. Sönmez)

Table Captions :

Table S1 The experimental and theoretical absorption wavelength (nm), excitation energies *E* (nm) and oscillator strengths (*f*) of N-(4-nitrophenyl)-2,2-dibenzoylacetamite) (NPDBA) in different solution and gas phase.

Table S2 Calculated net charges by mulliken population method and natural population analysis (B3LYP/6-311++G(d,p) level).

Table S3 Second-order perturbation theory analysis of Fock Matrix in NBO basis forN-(4-nitrophenyl)-2,2-dibenzoylacetamite) (NPDBA).

Table S4 Calculated dipole moments (μ), polarizability (α) and first hyper polarizability (β) components for the title compound.

Figure Captions:

Scheme S1 The view of the title compound.

Figure S1 Experimental FT-IR spectrum of title compound.

Figure S2 Experimental (a) ^{1}H and (b) ^{13}C chemical shift spectra of the title compound.

Figure S3 The solvent effect on UV-*Vis* spectra of the title compound in ethanol and methanol.

Table S1 The experimental and theoretical absorption wavelength (nm), excitation energies *E* (nm) and oscillator strengths (*f*) of N-(4-nitrophenyl)-2,2-dibenzoylacetamite) (NPDBA) in different solution and gas phase.

	Experimental	**TD-DFT/B3LYP 6-311++G(d,p)**	
	λ (nm)	***E*(nm)**	***f* (a.u.)**
Gas Phase		268.32	0.0329
		320.68	0.2015
Ethanol	245	273.51	0.0389
	325	345.79	0.6454
Methanol	245	273.62	0.0355
	325	345.91	0.6402

Table S2 Calculated net charges by mulliken population method and natural population analysis (B3LYP/6-311++G(d,p) level).

ATOM	**Mulliken charges**	**Natural charges (NPA)**	**ATOM**	**Mulliken charges**	**Natural charges (NPA)**
C1	-0.181	0.193	N1	0.172	-0.610
C2	0.459	-0.224	N2	-0.204	0.483
C3	-0.022	-0.163	O1	-0.204	-0.571
C4	-0.506	0.051	O2	-0.127	-0.535
C5	-0.358	-0.171	O3	-0.233	-0.614
C6	-0.145	-0.216	O4	-0.007	-0.390
C7	-0.286	0.706	O5	-0.007	-0.383
C8	0.634	-0.457	H1	0.449	0.435
C9	-0.191	0.595	H2	0.241	0.251
C10	0.455	-0.157	H3	0.255	0.242
C11	0.167	-0.139	H5	0.257	0.244
C12	-0.471	-0.199	H6	0.162	0.216
C13	-0.179	-0.164	H8	0.264	0.247
C14	-0.298	-0.201	H11	0.212	0.231
C15	-0.650	-0.165	H12	0.181	0.212
C16	-0.620	0.582	H13	0.168	0.210
C17	0.917	-0.167	H14	0.194	0.212
C18	0.450	-0.143	H15	0.066	0.208
C19	-0.306	-0.202	H18	0.222	0.229
C20	-0.430	-0.167	H19	0.187	0.211
C21	-0.362	-0.201	H20	0.164	0.209
C22	-0.869	-0.171	H21	0.205	0.212
			H22	0.178	0.229

Table S3 Second-order perturbation theory analysis of Fock Matrix in NBO basis forN-(4-nitrophenyl)-2,2-dibenzoylacetamite) (NPDBA).

Donor (*i*)	**E_D (*i*)(e)**	**Acceptor (*j*)**	**ED (*j*)(e)**	***E*(2)^a (kcal mol^{-1})**	***E(j)–E(i)*^{b} (a.u.)**	**F(*i. j*)^c (a.u.)**
n(O5—N8)	1.98639	LP (3) O4	1.45839	12.20	0.17	0.078
π(C9—C10)	1.60396	π*(C12—C14)	0.39112	25.31	0.28	0.075
		π*(C15—C17)	0.29168	16.34	0.28	0.062
π(C12—C14)	1.64626	π*(O5—N8)	0.63124	26.43	0.14	0.059
		π* (C9—C10)	0.37489	16.61	0.29	0.062
		π*(C15—C17)	0.29168	22.01	0.29	0.073
π(C15—C17)	1.68991	π*(C9—C10)	0.37489	21.51	0.28	0.071
		π*(C12—C14)	0.39112	17.30	0.28	0.064
π(C23—C32)	1.63887	π*(O1—C22)	0.15297	20.37	0.27	0.070
		π*(C24—C26)	0.27551	19.30	0.29	0.068
		π*(C28—C30)	0.31210	17.84	0.29	0.064
π(C24—C26)	1.64765	π*(C23—C32)	0.37946	19.08	0.28	0.065
		π*(C28—C30)	0.31210	21.74	0.28	0.070
π(C28—C30)	1.63903	π*(C23—C32)	0.37946	22.88	0.28	0.072
		π*(C24—C26)	0.27551	17.36	0.29	0.065
π(C35—C44)	1.63742	π*(O2—C34)	0.14425	19.31	0.27	0.068
		π*(C36—C38)	0.28130	19.78	0.29	0.069
		π*(C40—C42)	0.31254	17.74	0.28	0.064
π(C36—C38)	1.65083	π*(C35—C44)	0.37431	18.83	0.28	0.065
		π*(C40—C42)	0.31254	21.62	0.28	0.070
π(C40—C42)	1.64081	π*(C35—C44)	0.37431	22.82	0.28	0.072
		π*(C36—C38)	0.28130	17.61	0.29	0.065
LP (1)O1	1.97256	RY*(1) C22	0.01651	14.31	1.59	0.135
LP (2)O1	1.87542	σ*(N6—H7)	0.03851	6.87	0.69	0.063
		σ*(C20—C22)	0.06488	18.97	0.65	0.101
		σ*(C22— C23)	0.06139	18.47	0.72	0.105
LP (1)O2	1.97751	RY*(1) C34	0.01726	15.62	1.58	0.141
LP (2)O2	1.86875	σ*(C20—C34)	0.08202	24.33	0.60	0.109
		σ*(C34—C35)	0.06465	18.21	0.71	0.103
LP (1)O3	1.97608	RY*(1) C19	0.01599	15.95	1.69	0.147
LP (2)O3	1.85640	π*(N6—C19)	0.07112	23.94	0.72	0.120
		σ*(C19—C20)	0.06990	20.16	0.61	0.101
LP (1)O4	1.98192	RY*(1) N8	0.01752	5.87	1.91	0.094
		π*(N8—C14)	0.10216	4.21	1.08	0.061
LP (2)O4	1.90109	π*(O5—N8)	0.05460	18.88	0.72	0.106
		π*(N8—C14)	0.10216	11.87	0.57	0.074
LP (3)O4	1.45839	π*(O5—N8)	0.63124	160.60	0.14	0.138
LP (2)O5	1.90033	π*(O4—N8)	0.05512	19.00	0.72	0.106
		π*(N8—C14)	0.10216	11.94	0.57	0.074
LP (1)N6	1.62581	π*(O3—C19)	0.29793	63.22	0.27	0.119
		π*(C9—C10)	0.37489	38.06	0.29	0.094
n(O1-C22)	1.97577	π*(C23—C32)	0.37946	120.69	0.01	0.072
n(O2-C34)	1.97350	π*(C35—C44)	0.37431	128.68	0.01	0.070
n(O5-N8)	1.98639	π*(C12—C14)	0.39112	17.57	0.14	0.063

E_D means electron density.

[a] *E*(2) means energy of hyper conjugative interactions.

[b] Energy difference between donor and acceptor *i* and *j* NBO orbitals.

[c] *F(i, j)* is the Fock matrix element between *i* and *j* NBO orbitals.

Table S4 Calculated dipole moments (μ), polarizability (α) and first hyper polarizability (β) components for the title compound.

μ_x=-4.264a.u.	β_{xxx}=2644.054a.u.
μ_y=0.030a.u.	β_{xxy}=274.577a.u.
μ_z=-0.375a.u.	β_{xyy}=149.551 a.u.
μ_{tot}=4.281Debye	β_{yyy}=-522.722a.u.
α_{xx}=410.028a.u.	β_{xxz}=94.908 a.u.
α_{xy}=-11.047 a.u.	β_{xyz}=71.225 a.u.
α_{yy}=296.899a.u.	β_{yyz}=40.704 a.u.
α_{xz}=14.167a.u.	β_{xzz}=-168.439a.u.
α_{yz}=-36.727a.u.	β_{yzz}=8.389a.u.
α_{zz}=220.295a.u.	β_{zzz}= -55.916a.u.
α_{tot}=45.800 Å^3	β_{tot}=2.283x10^{-29} cm^5/esu

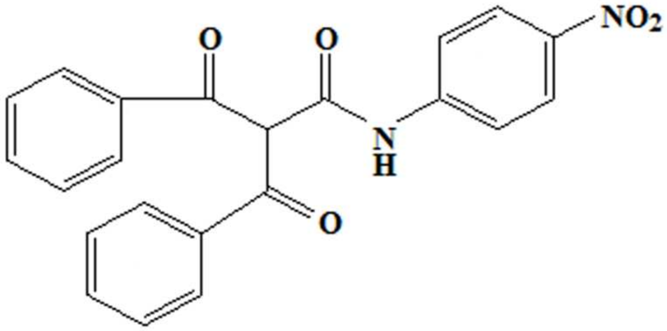

Scheme S1 The reaction for the synthesis of the title compound.

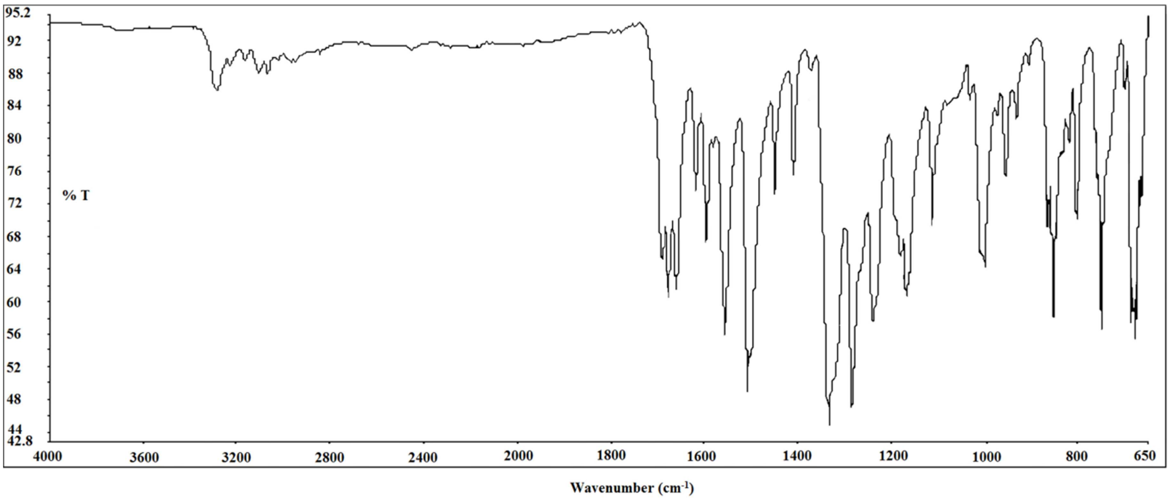

Figure S1 Experimental FT-IR spectrum of title compound.

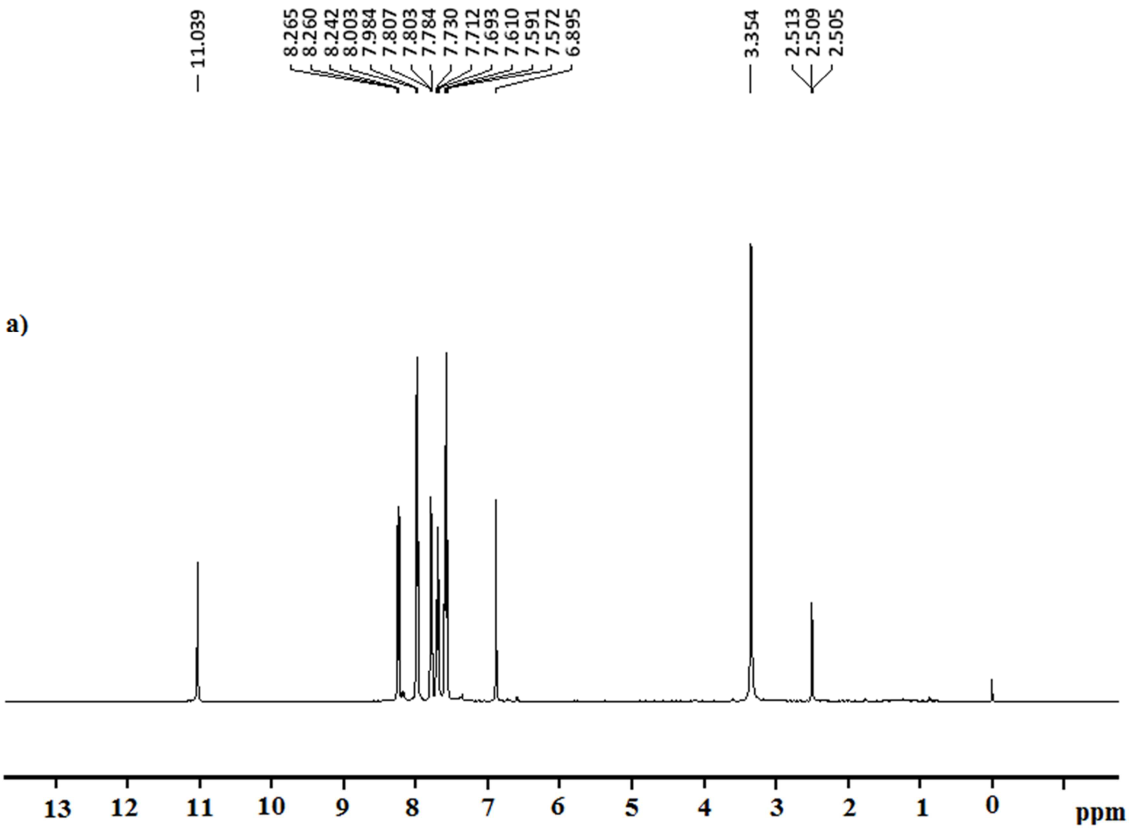

Figure S2 ^{1}H-NMR (DMSO-d6) spectrum of the title compound (with respect to TMS, all values ppm).

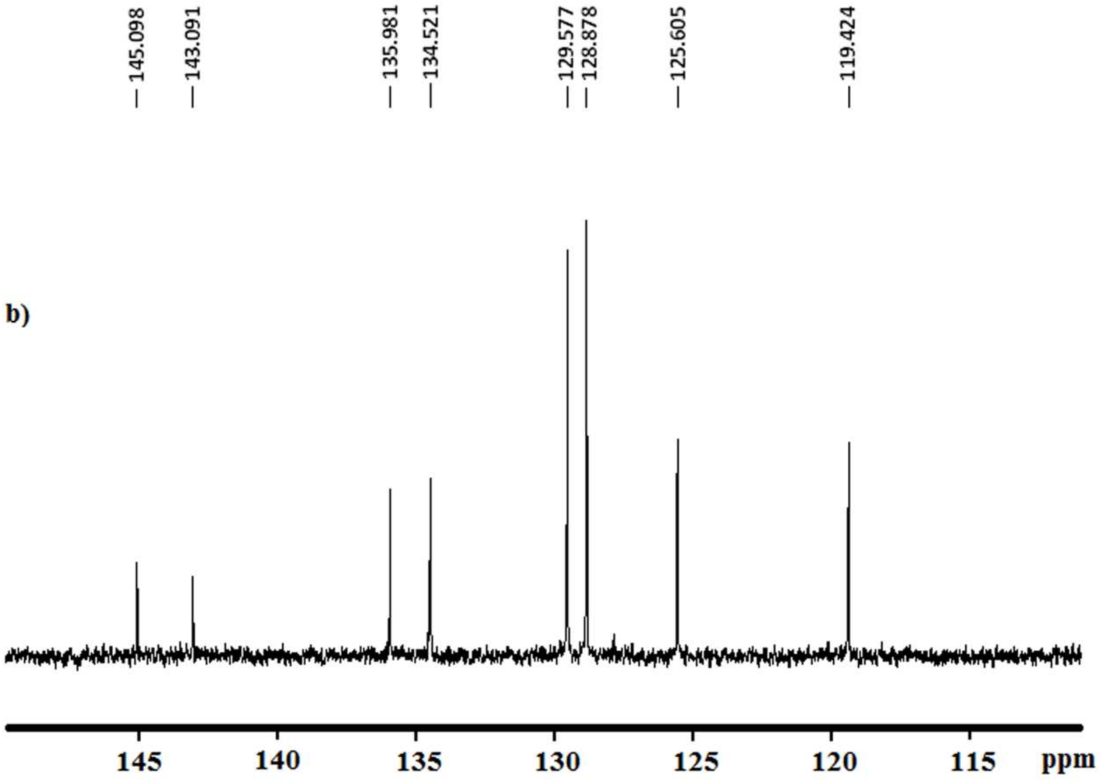

Figure S3 ^{13}C-NMR (DMSO-d6) spectrum of the title compound (with respect to TMS, all values ppm).

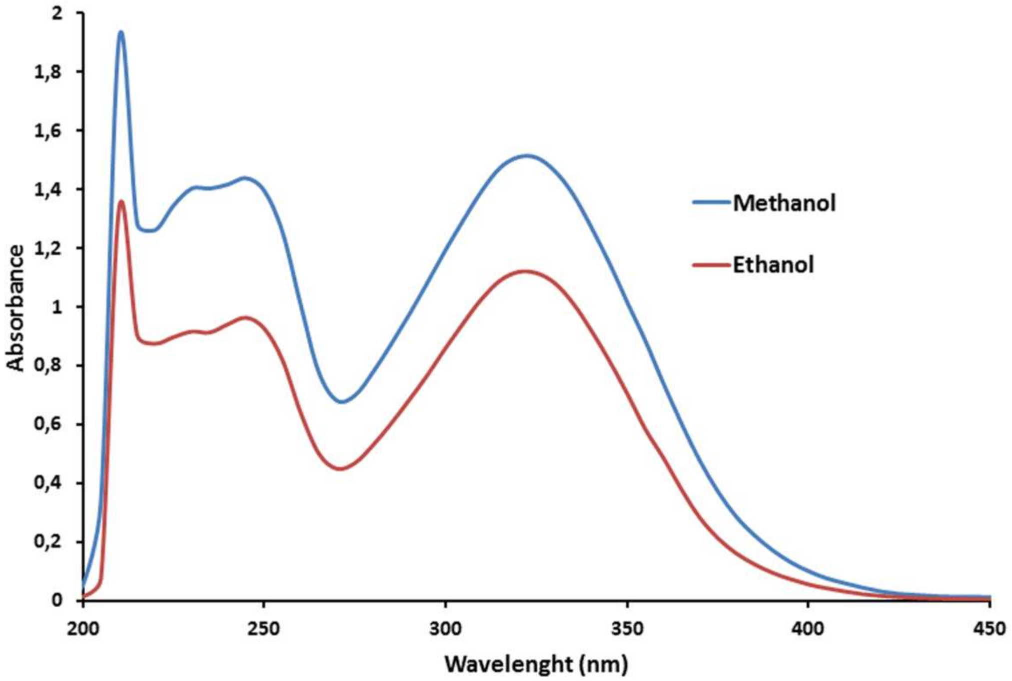

Figure S4 The solvent effect on UV-*Vis* spectra of the title compound in ethanol and methanol.